JOURNAL OF MATERIALS SCIENCE 18 (1983) 81–88

X-ray topographic investigations of dislocations in sodium chlorate

R. M. HOOPER*, K. J. ROBERTS‡, J. N. SHERWOOD
Department of Pure and Applied Chemistry, University of Strathclyde, Glasgow, Scotland, UK

Self-nucleation in saturated aqueous solutions of sodium chlorate leads principally to the formation of crystals of {1 0 0} habit which are highly perfect. Occasionally, crystals of the more complex form {1 0 0}, {1 1 0}, {1 2 0}, {1 1 1} can occur. These are more defective and highly strained. All crystals contain growth dislocation alignments characteristic of the growth sector within which they propagate as defined by a theoretical analysis. These are of edge, mixed and screw character and predominantly have Burgers vectors $a\langle 1\,0\,0\rangle$. Occasionally higher energy dislocations with Burgers vectors $a\langle 1\,1\,0\rangle$ are found. These are very few in number in crystals of the simple habit but occur more frequently in the multi-faceted crystals. The calculated line energy of the dislocations formed is less than about 100 eV nm^{-1}.

1. Introduction

The few previous X-ray topographic examinations of dislocations in sodium chlorate crystals have shown a variety of dislocation distributions and sources. Kito and Kato [1] noted two basic types of dislocations in self-nucleated crystals; these initiated at the nucleus and at the inclusions incorporated during growth. Both types were observed to propagate normal to the {1 0 0} crystal faces. In an earlier paper, Mussard and Goldsztaub [2] demonstrated that the latter type can also nucleate at points on the growing crystal surface where localized regions of excessive supersaturation develop. More recently, Matsunaga *et al.* [3] have examined the influence of gross dislocation substructure on the rate and mechanism of the growth of small, seeded crystals. The defect structure of these last crystals was dominated by large numbers of dislocations generated at the seed–crystal interface and which propagate into the growing crystal. In all three publications, an effort was made to define the geometry of the defects but this was not carried out in detail, particularly with respect to the self-nucleated crystals. We have carried out an examination of both growth and mechanically-induced dislocations in self-nucleated and seeded crystals grown from an aqueous solution, and of the relationship between the defect structure and crystal morphology. The present paper describes the basic theoretical background and compares the results with the observed dislocation configurations in the self-nucleated crystals. It is developed to an examination of the generation of dislocations during thermal treatment and incipient decomposition in an accompanying paper [4]. Future publications will deal with dislocation distributions and dislocation geometries in seeded and impure crystals.

2. Theoretical analysis

At room temperature, sodium chlorate is primitive cubic space group $P2_13$, with $a_0 = 0.67756$ nm and four $NaClO_3$ to the unit cell [5]. The structure resembles that of NaCl but the expansion of the lattice to accommodate the larger, anisotropic, ClO_3^- ion results in the loss of the symmetry of this structure. The principal effect of this in the present context is to remove the possibility of slip

*Present address: Department of Engineering Science, University of Exeter, Stocker Road, Exeter, UK.
‡Present address: Institut fur Kristallographie, RWTH, Templergraben, 55, D-5100 Aachen, West Germany.

0022–2461/83/010081–08$03.46/0

by $a/2\langle 1\,1\,0\rangle$ which dominates in the NaCl structure, leaving the most likely Burgers vectors, **b**, of dislocations as

$$a\langle 1\,0\,0\rangle, 0.658\,\text{nm}; \qquad a\langle 1\,1\,0\rangle, 0.930\,\text{nm};$$

$$a\langle 1\,1\,1\rangle, 1.139\,\text{nm}.$$

The energy of a linear dislocation comprises two terms; the line tension energy E_l and the core energy. The latter contribution is relatively small and is usually ignored. The former is given by [6, 7]

$$E_l = ck|\mathbf{b}|^2$$

where c is a constant which depends on the crystal structure. The energy factor, k, reflects the elastic properties of the crystal around the line direction and $|\mathbf{b}|$ is the modulus of the Burgers vector. The last term dominates, thus, dislocations with Burgers vectors $a\langle 1\,0\,0\rangle$ and $a\langle 1\,1\,0\rangle$ will be of the lowest energy and hence most likely to occur.

The elastic constants for sodium chlorate are ($/10^{10}$ Nm^{-2}) [8]

$$c_{11} = 4.92, \quad c_{12} = 1.42 \quad \text{and} \quad c_{44} = 1.16$$

The anisotropy factor, $A = (c_{11} + c_{12})/2c_{44} = 1.51$ indicates that the system is moderately isotropic. From this data we evaluate k and E_l for the two shortest Burgers vectors (Table I). The dislocation of the lowest line energy is that with $\mathbf{b} = a\langle 1\,0\,0\rangle$ in the screw configuration: $E_l = 41\,\text{eV nm}^{-1}$, compared with $E_l = 12\,\text{eV nm}^{-1}$ for $\mathbf{b} = a/2\langle 1\,1\,0\rangle$ in sodium chloride. This distinction in energy is reflected in the bulk properties of the material. We have found it impossible to induce widespread slip in $NaClO_3$ at 295 K ($T/T_m \simeq 0.5$, melting point, $T_m = 535$ K); fracture occurs before slip. The plastic properties of sodium chloride at these temperatures ($T/T_m = 0.3$) are well known.

Analysis of growth dislocation configurations in crystals grown from solution [6, 7] have shown that these dislocations inevitably propagate along a small number of specific directions in any particular growth sector. The directions are defined as being those along which the elastic line energy per unit length, $W = k/\cos\alpha$, is a minimum and where α is the angle between the growth direction (normal to the growth sector facet), **n**, and the dislocation line direction, **l**.

Sodium chlorate crystallizes from aqueous solution with a dominant $\{1\,0\,0\}$ habit, sometimes modified by the presence of $\{1\,1\,0\}$, $\{1\,1\,1\}$ and $\{1\,2\,0\}$ forms [9]. Evaluation of k and its minimization with respect to α for dislocations with $a\langle 1\,0\,0\rangle$ and $a\langle 1\,1\,0\rangle$ Burgers vectors in all the resulting growth sectors leads to the data tabulated in Table II. Table II includes, in addition to the terms already defined in the text, the multiplicities of a particular crystal growth form, $M(\mathbf{n})$, and of a particular dislocation type, $M(\mathbf{l})$; the percentage screw charater of the dislocation, $S(\mathbf{l})$, and its percentage component along the growth direction, $S(\mathbf{n})$, and the plane containing the line direction and Burgers vector of the dislocation, the composition plane, $C(h\,k\,l)$.

TABLE I Values of the energy factor ($k/10^{10}$ Nm^{-2}) and line energy (E_l/eV nm^{-1}) for dislocations of $\mathbf{b} = a\langle 1\,0\,0\rangle$ and $\mathbf{b} = a\langle 1\,1\,0\rangle$ in sodium chlorate

b	Screw		Edge			
	k	E_l	Minimum		Maximum	
			k	E_l	k	E_l
$a\langle 1\,0\,0\rangle$ 0.658 nm	1.160	41	1.932	68	1.957	69
$a\langle 1\,1\,0\rangle$ 0.930 nm	1.425	100	1.812	127	1.957	137

3. Experimental details

3.1. Crystal preparation

Self-nucleated crystals of sodium chlorate were prepared by the slow, controlled, evaporation of saturated, aqueous, solutions of the multiple, recrystallized, Analar solid at 298 K. The resulting crystals, the lower surface of which was in contact with mercury during growth, were free from visible imperfections.

For the most part, the crystals (about 1 cm × 1 cm × 0.2 cm) were of square or rectangular habit bounded by $\{1\,0\,0\}$ facets. Occasionally, crystals formed additional $\{1\,1\,0\}$, $\{1\,2\,0\}$ and $\{1\,1\,1\}$ facets. Crystals of the latter habit were, visibly, much less perfect.

3.2. X-ray topography

X-ray transmission topographs [10] of the complete crystals were taken using AgKα ($\mu_0 t$ about 1.3) radiation and were recorded on Ilford L4 nuclear plates. In the more perfect crystals well-contrasted topographs could be produced from 200, 120 and 111 type reflections; 220 reflections yielded topographs of lower, but recognizable definition. In crystals of low perfection, only 200 type reflections yielded adequately resolved dislocation images.

TABLE II Calculated line directions and line energies for dislocations with {100} and {110} Burgers vectors in the various growth sectors of sodium chlorate

Type	n	M(n)	b	M(b)	b	l	M(l)	Character	S(l)	S(n)	α(l, n)	$C(h\,k\,l)$	E_l (eV nm^{-1})
1a	(100)	6	[100]	6	0.66	[100]	2	Screw	100.0	100.0	0.0	None	40.7
1b	(100)	6	[010]	6	0.66	[100]	4	Edge	0.0	0.0	0.0	(001)	68.6
1c	(100)	6	[110]	12	0.93	[510]	8	Mixed	82.9	70.7	11.0	(001)	104.3
1d	(100)	6	[011]	12	0.93	[100]	4	Edge	0.0	0.0	0.0	(01$\bar{1}$)	137.3
2a	(110)	12	[100]	6	0.66	[310]	4	Mixed	94.6	70.7	26.0	(001)	44.8
2b	(110)	12	[001]	6	0.66	[110]	2	Edge	0.0	0.0	0.0	($\bar{1}$10)	67.8
2c	(110)	12	[110]	12	0.93	[110]	2	Screw	100.0	100.0	0.0	None	99.9
2d	(110)	12	[101]	12	0.93	[531]	8	Mixed	72.0	50.0	17.1	($\bar{1}$11)	114.5
2e	(110)	12	[110]	12	0.93	[110]	2	Edge	0.0	0.0	0.0	(001)	127.1
3a	(111)	8	[001]	6	0.66	[113]	6	Mixed	89.9	57.7	28.7	(1$\bar{1}$0)	47.8
3b	(111)	8	[110]	12	0.93	[995]	6	Mixed	93.4	81.6	14.3	(1$\bar{1}$0)	105.9
3c	(111)	8	[$\bar{1}$10]	12	0.93	[111]	6	Edge	0.0	0.0	0.0	(11$\bar{0}$)	128.6
4a	(120)	12	[010]	6	0.66	[160]	2	Mixed	98.8	89.4	17.6	(001)	41.7
4b	(120)	12	[001]	6	0.66	[120]	2	Edge	0.0	0.0	0.0	($\bar{2}$10)	68.0
4c	(120)	12	[100]	6	0.66	[430]	2	Mixed	52.5	44.7	27.4	(001)	80.9
4d	(120)	12	[110]	12	0.93	[590]	2	Mixed	96.1	94.9	2.4	(001)	100.5
4e	(120)	12	[011]	12	0.93	[3102]	4	Mixed	80.2	63.2	15.2	(2$\bar{1}$1)	107.4
4f	(120)	12	[101]	12	0.93	[451]	6	Mixed	55.0	31.6	15.3	($\bar{2}$12)	124.7

4. Results and discussion

4.1. Dislocation configurations

4.1.1. Crystals with {100} habit

Topographs of the three most generally found dislocation distributions in {100} facetted crystals are shown in Figs. 1 to 3. We classify these as follows:

(A) Single dislocations emanating from the nucleus of the crystals (X, in all figures).

(B) Single dislocations which nucleate at inclusions in growth sectors or on growth sector boundaries.

(C) Groups of dislocations nucleating at linear inclusions within the growth sectors (e.g. Y in all figures).

(D) Fans of dislocations nucleating at point inclusions (Fig. 3).

(E) Single dislocations or parts of dislocations which do not appear to lie normal to the facet of the growth sector in which they nucleate (Z, Figs. 1, 2 and 3).

Dislocations of types A, B and C all appear to propagate normal to the crystal facet which bounds the growth sector which contains them.

Additional features which are worthy of note are the fringe patterns F in the growth sectors (these are particularly noticeable in Fig. 1) and the small strain marks (e.g. S, Fig. 1). Both show a change in contrast with variation of the diffraction vector **g**. The former have been noted previously by Kito and Kato [1] and were ascribed by them to a lattice twist across the growth sector boundary. The latter, although few in the example given, are numerous in rapidly grown crystals. They can be attributed to isotropic strain built up around point inclusions (impurity, solvent or vacancy clusters) in the lattice. Presumably the resulting strain is insufficient to generate dislocations. The growth sector boundaries vary considerably in contrast from crystal to crystal. In some cases (e.g. Fig. 3) they are well contrasted indicating a high degree of mismatch between the lattice in the adjacent sectors. In other cases (Fig. 1) the boundaries are only noticeable from the absence or change in orientation of the fringe patterns.

Dislocations of types A, B and C form by far the dominant type of alignment. That **l** is parallel to **n** for these dislocations is well defined by the 111 type reflection (Fig. 1c). Even in this projection all dislocations remain rigidly parallel to the ⟨100⟩ axes of the crystal. Reference to Table II will show that these must be dislocations of the types 1a, 1b or 1d of pure screw or edge character. Comparison of the 200 and 020 reflections is sufficient to confirm that this is the case. The most striking confirmation is for the screw dislocation which propagates along the long, [010] axis of the crystal. This is well imaged in Fig. 1a but goes out of contrast completely, in Fig. 1b. The numerous other absences in Fig. 1b of dislocations with

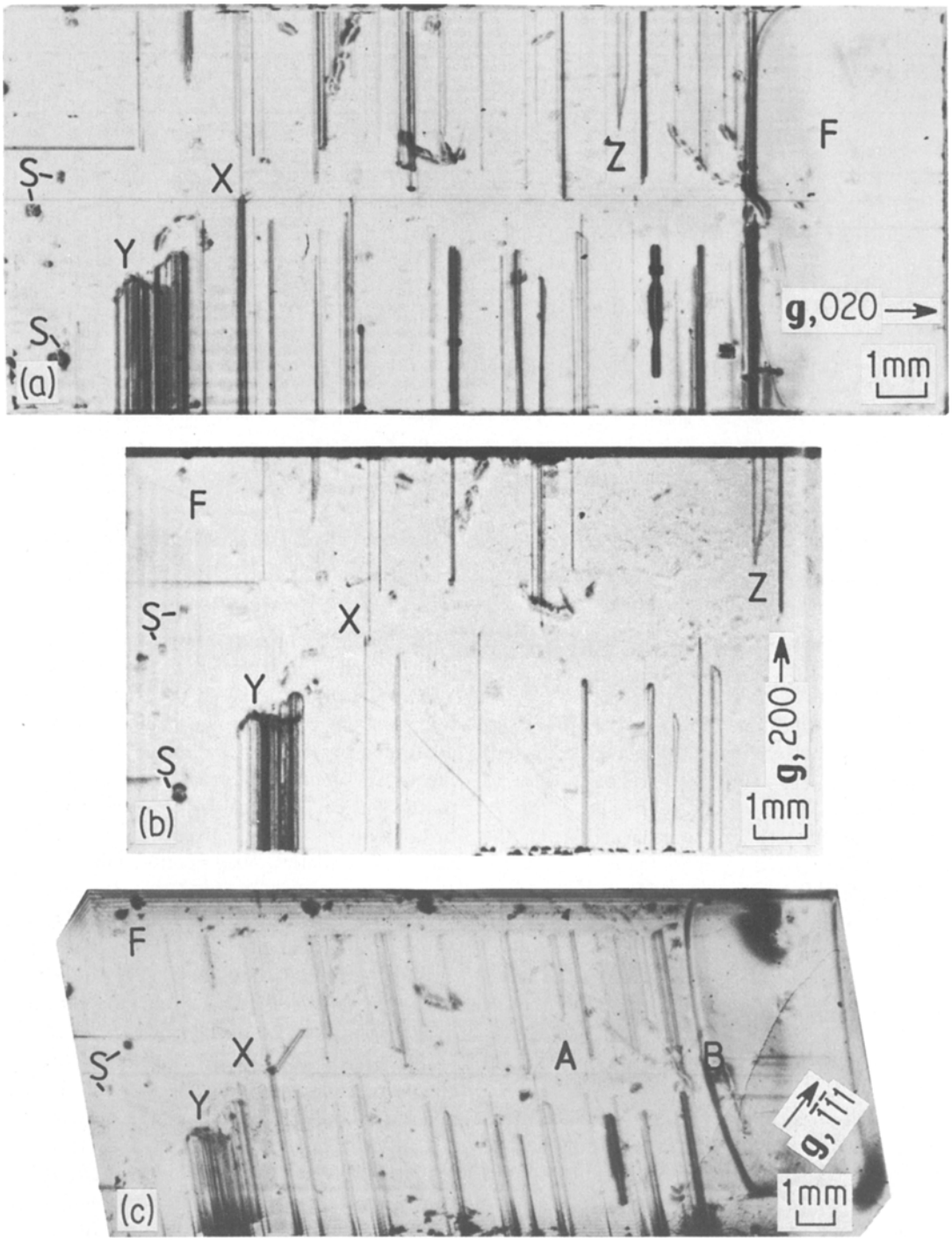

Figure 1 X-ray transmission topographs of a sodium chlorate crystal of elongated {1 0 0} habit (AgKα). (a) 0 2 0 reflection, (b) 2 0 0 reflection and (c) $\bar{1}\,\bar{1}\,1$ reflection. The crystal fractured before the topograph in Fig. 1b was obtained. Its relationship to the other topographs is obvious. The light portion at the right hand end of Figs. 1a and c was obscured by the crystal mount.

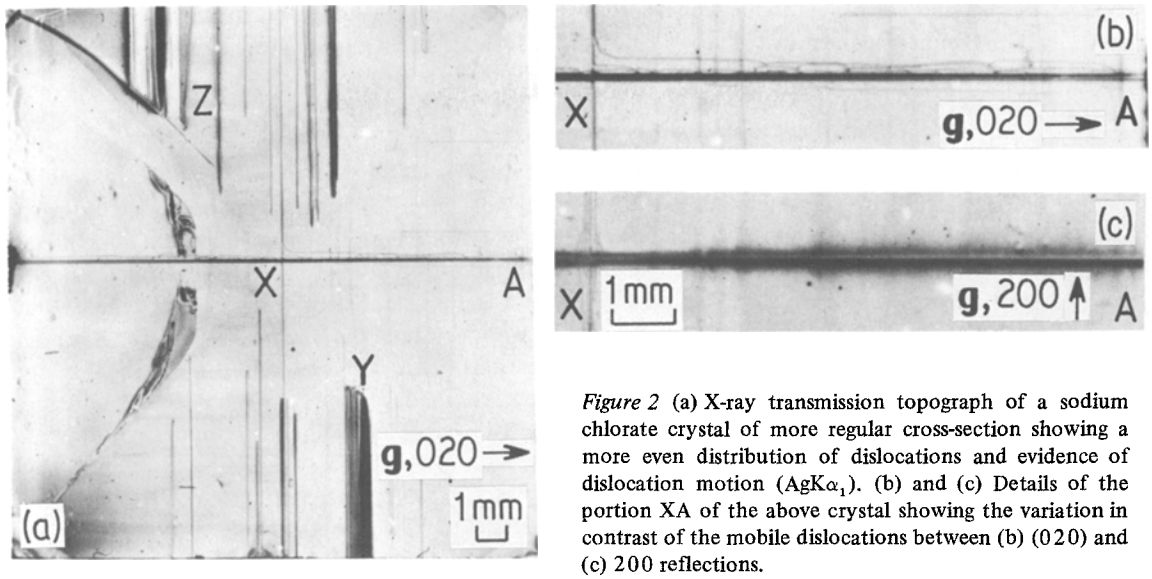

Figure 2 (a) X-ray transmission topograph of a sodium chlorate crystal of more regular cross-section showing a more even distribution of dislocations and evidence of dislocation motion ($AgK\alpha_1$). (b) and (c) Details of the portion XA of the above crystal showing the variation in contrast of the mobile dislocations between (b) (020) and (c) 200 reflections.

$1 = [100]$ define these as pure edge dislocations.

In the (100) growth sector, these edge dislocations may have Burgers vectors [010], [001], $[0\bar{1}1]$ or [011]. Of these the first two have by far the lowest line energy (Table I). Additionally, the examination of a wide range of reflections (200, 020, 120, $\bar{1}$10, 220 etc.) failed to reveal the variation in image contrast which would be expected for edge dislocations with [011] type Burgers vectors. Consequently, we conclude that the observed type A images are of dislocations of the types ⟨100⟩ screw and ⟨100⟩{010} edge (types 1a and 1b, Table II).

In slowly grown, self-nucleated crystals most dislocations of these types remain sessile and propagate linearly. It is not uncommon however to find evidence of dislocation migration [1]. This is particularly noticeable in Fig. 2 where some type A dislocations of screw character have looped out of the linear configuration. The sides of these loops lie along the [100] and [010] directions in the (001) plane and their presence and absence in the two reflections (Figs. 2b and c) define them as looping from an edge to a screw character. Such behaviour is usually ascribed to dislocation slip. We find it strange that this should happen in such a brittle material as sodium chlorate which, as we have noted above, does not undergo slip at the growth temperature even under considerable mechanical constraint. It may be that excessively large stresses are built up during growth and which facilitate this. Certainly, as we shall show elsewhere [12] such configurations are more common in rapidly grown, seeded crystals which may be more highly stressed during growth. Alternatively, such behaviour could result from climb due to the trapping of an excess of point defects at the solid/solution interface during growth and which would then diffuse to dislocation sinks within the crystal. More rapid growth could trap increased numbers of these defects and hence a similar parallel between the amount of climb and the growth rate could result. Support for the latter mechanism has been found in the observation of dislocation

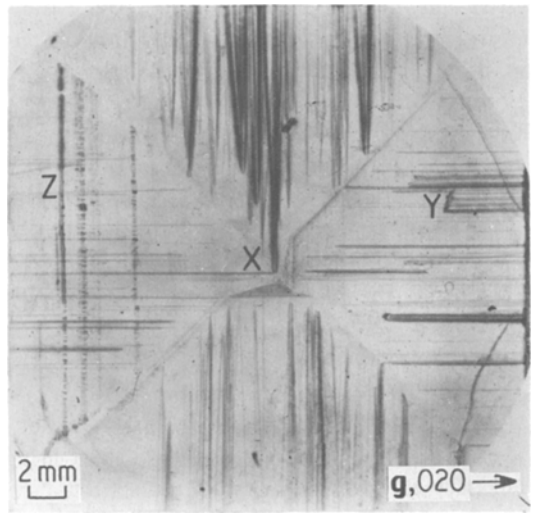

Figure 3 X-ray transmission topograph of a sodium chlorate crystal of simple habit containing a large number of dislocation fans ($AgK\alpha$). The round corners are defined by the crystal mount.

helices in crystals of α-sulphur grown from solution at ambient temperatures [11].

Additional to those defects which show the variation in contrast from 020 to 200 reflection there are many apparently single, type B dislocations and type C bundles which show no change of contrast. It is tempting to define these as dislocations of mixed character. The theoretical calculations (Table II) indicate however that the most likely such dislocation to occur in a (100) growth sector, ($\mathbf{b} = a[110]$), should lie at 11° to the growth vector **n** (approximately ⟨510⟩). Since a few such orientations are noticeable (designated type E) e.g. Z in Figs. 2 and 3 we conclude that this theoretical prediction is valid and confirms the existence of this type of dislocation. On this basis, we can only conclude that those images which do not change in contrast in Figs. 1 and 2 are bundles of pure screw and edge dislocations; the one being in contrast whilst the other is absent and vice versa.

The final type of image is that designated as type D, fans of dislocations, which are most noticeable in Fig. 3. We have no doubt that these represent dislocation bundles. They differ from type C images in that they are generated at a point inclusion rather than at a line inclusion. The fanning then results from dislocation–dislocation repulsion. It is interesting to note that many of these diverge to an equilibrium distance whereafter they continue to propagate parallel to **n**.

Finally it is interesting to note the relationship between the distribution of dislocations in these crystals and the habit. Due to the method of preparation (on a surface) growth in the $[00\bar{1}]$ direction is inhibited and only the remaining growth sectors can propagate. The (001) sector is always the most perfect and most slowly growing. Reference to Fig. 1c will show that there are at most three dislocations (X, A and B) which propagate in this sector. X and A are just discernable in Fig. 1a and hence they are not screw dislocations.

In contrast, the more defective sectors propagate more rapidly. Where similar densities of dislocations exist, the rates of growth are more or less equivalent to yield the square cross-section of Figs. 2 and 3. The crystal in Fig. 1 does not fit this pattern. The most rapidly growing (010) sectors contain a similar dislocation density to the (001) sector but advance at a much greater rate (about 40×). We ascribe this to the single and presumably powerful screw dislocation lying along the axis of this crystal and note that we have found a similar correlation between screw dislocations and rapidly growing sectors for several other solids.

We conclude, on theoretical and experimental grounds that the dominant types of growth dislocation in {100} growth sectors of sodium chlorate are pure screw and edge dislocations of $\mathbf{b} = a\langle 100\rangle$. There is tentative evidence for mixed dislocations of $\mathbf{b} = a\langle 110\rangle$. The lower incidence of these is consistent with their increased line energy relative to the types 1a and 1b (see Table II) dislocations. This supports our contention that the more energetic type 1d (Table II) dislocations (**b**[011], edge) are unlikely to occur.

4.1.2. Crystals with {100}, {110}, {120} and {111} habit

Although most self-nucleated crystals were of the simple {100} form, crystals of a more complicated morphology were occasionally found. In addition to the {100} growth sectors, these also contained well defined {100}, {120} and {111} growth sectors [9]. Topographs of such crystals showed them to be more defective than crystals of the simple habit. There is some evidence to support the contention that this crystal form results from the further growth of damaged crystals of simple habit. For example, this is a common form of larger crystals prepared by seeded growth where damage to the seed crystal surface propagates with the growing crystal [12].

Fig. 4 shows a composite topograph (020 reflection) of a thin crystal of this habit. The considerable increase in disorder and strain in this type of crystal compared with those of the simple form is immediately apparent. The distortion of the crystal was so great that it was not possible to image the crystal on a single topograph. Even on the separate parts, half is less well contrasted than the remainder. It proved impossible to characterize the dislocations in the new growth sectors by orientation contrast. The combination of lattice strain plus the increased image widths in reflections other than 200 types yielded diffuse images which could be used, at best, to help define the principal line directions of dislocations in some regions. Comparison of these line directions with those predicted by the theoretical analysis is used to indicate the possible character of the dislocations.

On the right hand edge a thin (011) growth sector overlies the (010) sector. The few dis-

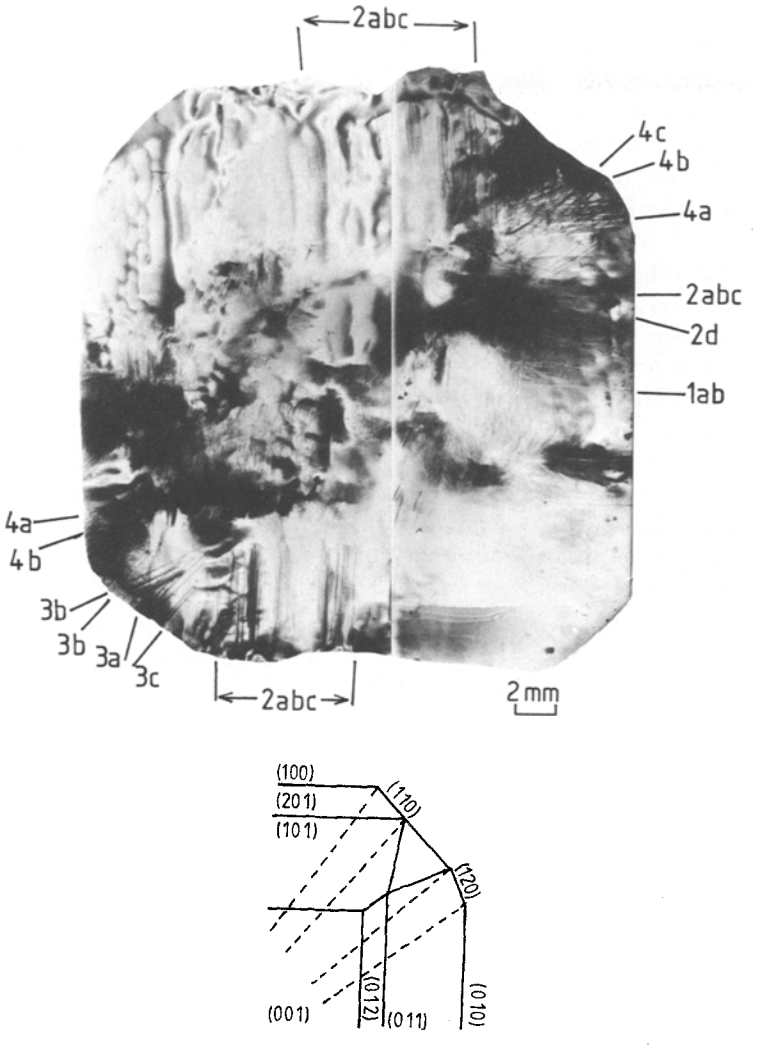

Figure 4 (a) X-ray transmission topograph of a sodium chlorate crystal of more complex habit showing the considerable degree of strain and imperfection in this type of crystal (AgKα). (b) Approximate position of the growth sectors in this crystal.

locations terminating at the surface most likely lie in the (010) sector and are of the types described in section 4.1. Those terminating within the image will lie in the (011) sector. These are of two orientations [010] and [153]. The latter orientation probably corresponds to type 2d (Table II) mixed dislocations with **b**[101] (Table I) and are so designated in Fig. 4. The former could be of types 2a, b, c or e (Table II) all of which would show this projected alignment. Some resolution of these can be obtained from the alignments of the dislocations in the upper, (101), growth sector. Here the images follow the [301], [103] and [101] directions. The former confirm the presence of the low energy mixed dislocations type 2a, **b**[100]. No definition of the dislocation with [101] projected orientation can be given (i.e. 2b, c, or e) since variation of **g** failed to yield any definite variation of contrast with which to define these.

The (120) growth sector contains four dislocation alignments which can be assigned line directions corresponding to dislocations of types 4a, b, c and d. Those of type 4a are distinctive and this assignment is definitive. There is no doubt that there are a group of dislocations which lie approximately both normal to the (120) face and at a slight angle to this direction. This would be consistent with the alignments expected for 4b and 4d. These dislocations show evidence of mobility during growth. The final orientation we assign to 4c simply because this has the lowest energy of the remaining predictions. Otherwise dislocations of types 4e and 4f cannot be ruled out. A change in alignment noticeable in a less well contrasted 111 reflection (not presented) does support a type 4c alignment.

The (111) growth sector is largely obscured by the defective area. Within this, alignments corresponding to a $[\bar{1}22]$ orientation can be distinguished. The $(\bar{1}\bar{1}1)$ sector is more satisfactorily

imaged. In this we can define line directions corresponding to dislocation types 3a, b and c.

Although tentative, this analysis confirms the existence of dislocation alignments in the various growth sectors consistent with the theoretical predictions. A more detailed analysis of these additional growth sectors in seeded crystals is presently in progress [12].

As noted for the crystals of simple habit, the dislocations observed have Burgers vectors which are predominantly $a\langle 1\,0\,0\rangle$. Dislocations with $\mathbf{b} = a\langle 1\,1\,0\rangle$ occur with greater frequency. This no doubt results from the increased strain developed in the crystals as they grow with this habit.

Acknowledgements

We gratefully acknowledge the financial support of SERC through the award of apparatus grants (JNS) and Research Assitantships (RMH and KJR).

References

1. I. KITO and N. KATO, *J. Cryst. Growth* **24/25** (1974) 544.
2. F. MUSSARD and S. GOLDSZTAUB, *ibid.* **13/14** (1972) 445.
3. M. MATSUNAGA, M. KITAMURA and I. SUNAGAWA, *ibid.* **48** (1980) 425.
4. I. D. BEGG, P. J. HALFPENNY, R. M. HOOPER, R. S. NARANG, K. J. ROBERTS and J. N. SHERWOOD, unpublished work.
5. G. R. RAMACHANDRAN and K. J. CHANDRASEKARAR, *Acta Cryst.* **10** (1957) 671.
6. H. KLAPPER, *Phys. Stat. Sol.(a)* **14** (1972) 99, 443.
7. Y. EPELBOIN, A. ZARKA and H. KLAPPER, *J. Cryst. Growth* **20** (1973) 103.
8. R. VISWANATHANY, *J. Appl. Phys.* 37 (1966) 884.
9. H. E. BUCKLEY, *Z. Krist.* 75 (1930) 15.
10. A. R. LANG, in "Diffraction and Imaging Techniques in Materials Science", 2nd edn. Edited by S. Amelincx, R. Gevers and J. Van Landuyt (N. Holland, Amsterdam, 1978) p. 449.
11. R. M. HOOPER and J. N. SHERWOOD, *Phil. Mag. A* (1982) in press.
12. K. J. ROBERTS and J. N. SHERWOOD, unpublished work.

Received 12 May
and accepted 26 May 1982